

# The superorbital variability and triple nature of the X-ray source 4U 1820{303

Andrzej A. Zdziarski,<sup>1?</sup> Linqing Wen,<sup>2,y</sup> and Marek Gierlinski<sup>3,4,z</sup>

<sup>1</sup>Centrum Astronomiczne im. M. Kozminki, Bartycka 18, 00-716 Warsaw, Poland

<sup>2</sup>Max-Planck-Institut für Gravitationsphysik, Albert-Einstein-Institut, Am Mühlenberg 1, D-14476 Golm, Germany

<sup>3</sup>Department of Physics, University of Durham, Durham DH1 3LE, UK

<sup>4</sup>Observatorium Astronomiczne Uniwersytetu Jagiellońskiego, Orla 171, 30-244 Krakow, Poland

26 May 2019

## ABSTRACT

We perform a comprehensive analysis of the superorbital modulation in the ultracompact X-ray source 4U 1820{303, consisting of a white dwarf accreting onto a neutron star. Based on RXTE data, we measure the fractional amplitude of the source superorbital variability (with a 170-d quasi-period) in the folded and averaged light curves, and find it to be by a factor of 2. As proposed before, the superorbital variability can be explained by oscillations of the binary eccentricity. We now present detailed calculations of the eccentricity-dependent flow through the inner Lagrangian point, and find a maximum of the eccentricity of  $\sim 0.004$  is sufficient to explain the observed fractional amplitude. We then study hierarchical triple models yielding the required quasi-periodic eccentricity oscillations through the Kozai process. We find the resulting theoretical light curves to match well the observed ones. We constrain the ratio of the semi-major axes of the outer and inner systems, the component masses, and the inclination angle between the inner and outer orbits. Last but not least, we discover a remarkable and puzzling synchronization between the observed period of the superorbital variability (equal to the period of the eccentricity oscillations in our model) and the period of the general-relativistic periastron precession of the binary.

**Key words:** accretion, accretion discs { binaries: general { globular clusters: individual: NGC 6624 { stars: individual: 4U 1820{303 { X-rays: binaries { X-rays: stars.

## 1 INTRODUCTION

4U 1820{303 is one of the most remarkable low-mass X-ray binaries. This ultracompact binary consists of an  $M_2 = (0.06 \pm 0.08)M_\odot$  He white dwarf secondary (Rappaport et al. 1987, hereafter R87) accreting via Roche-lobe overflow onto a neutron star (of the mass  $M_1$ ). Its binary period is as short as  $P_1 = 685$  s (Stella, Priedhorsky & White 1987; Anderson et al. 1997). A likely scenario for the formation of 4U 1820{303 appears to be a direct collision of a neutron star and a giant (Verbunt 1987; Ivanova et al. 2005) in its parent globular cluster NGC 6624. This resulted in a binary consisting of the neutron star and the stripped giant core, which then took  $10^6$  yrs to cool to the present almost-degenerate state (R87). The secondary has to have a very low H abundance in order to fill its Roche lobe (R87), and the

occurrence of type-I X-ray bursts implies that it cannot be made of elements heavier than He. Interestingly, 4U 1820{303 was the first X-ray burster identified with a known X-ray source (Ghoshal et al. 1976). The most likely distance to the source appears to be  $7.6 \pm 0.4$  kpc (Kuulkers et al. 2003), as discussed in a companion paper (Zdziarski, Gierlinski & Wen 2007, hereafter ZGW07).

The accretion occurs as a consequence of the loss of the angular momentum of the binary via emission of gravitational radiation (Paczynski 1967), as proposed for this system by Stella et al. (1987) and Verbunt (1987), and calculated in detail by R87. The implied present mass-loss rate from the secondary (R87; see Section 3 below) is completely compatible with that corresponding to the average isotropic bolometric luminosity measured from the Rossi X-ray Imaging Explorer (RXTE) data by ZGW07. This provides a strong support for this accretion model. The present phase of the high mass transfer started only  $10^6$  yrs ago and may be sustained only for  $3 \pm 10$  yrs (R87).

The 685-s period was discovered in X-rays as a modu-

<sup>?</sup> E-mail: aaz@camk.edu.pl

<sup>y</sup> E-mail: lwen@aeim pg.de

<sup>z</sup> E-mail: Marek.Gierlinski@durham.ac.uk

lation with a 2.3 percent peak-to-peak amplitude (Stella et al. 1987). The period is very stable, with a low  $P_1 = P_2 = (3.5 \pm 1.5) \times 10^8$  yr<sup>1</sup> (Chou & Grindlay 2001, hereafter CG 01), which makes it certain it is due to the binary motion. The modulation was proposed to be due to the obscuration of the X-ray source by a structure at the edge of the accretion disk. A stronger modulation in the UV was predicted by Atteas & King (1997), and subsequently discovered by Anderson et al. (1997), with  $P_1 = 687.6 \pm 2.4$  s and a 16 percent peak-to-peak amplitude.

The most unusual feature of 4U 1820-303 appears to be the luminosity variation by factor of  $> 2$  at a (superorbital) period of  $P_3 = 170$  d (Priedhorsky & Terrell 1984; Smale & Lochner 1992; CG 01; Simon 2003; Wen et al. 2006, hereafter W 06). CG 01 found the modulation is stable with  $P_3 = 171.0 \pm 0.3$  d and  $P_3 = P_2$   $< 2.2 \times 10^4$  yr<sup>1</sup> based on data from 1969 to 2000. W 06 found  $P_3 = 172 \pm 1$  d based on 8.5 yrs of RXTE All-Sky Monitor (ASM) data. The fact that X-ray bursts take place only at the flux minimum (Cornelisse et al. 2003, ZGW 07) proves that the observed variability is due to intrinsic luminosity/accretion rate changes and not due to, e.g., obscuration or changes of the projected area of the source due to precession. This is further supported by strong correlations between the observed flux and the source spectral state, varying with the flux in a way typical of atoll-type neutron-star binaries (Bloser et al. 2000; Gladstone, Done & Gierlinski 2007), and between the frequency of kHz QPOs observed from the source and the flux (Zhang et al. 1998; van der Klis 2000). The source was classified as an atoll by Hasinger & van der Klis (1989).

The intrinsic, accretion-rate related, character of the long-term periodic flux changes in 4U 1820-303 is unique among all sources showing superorbital variability. In other cases, such changes of the observed flux appear compatible with being caused by accretion disc and/or jet precession, which either results in variable obscuration of emitted X-rays as in Her X-1 (Katz 1973), or changes the viewing angle of the presumed anisotropic emitter, as in SS 433 (Katz 1980) or Cyg X-1 (e.g., Lachowicz et al. 2006), or both. However, that precession keeps the inclination angle of the disc with respect to the orbital plane constant, and thus it cannot change the accretion rate (or the luminosity). Also, the ratio between the superorbital and orbital periods is  $> 2.2 \times 10^4$ , which is much higher than that possible to obtain from any kind of disc precession at the mass ratio of the system (e.g., Larwood 1998; Wijers & Pringle 1999). This appears to rule out also models which would attempt to explain the variable accretion rate by a varying disc inclination angle (with respect to the orbital plane).

In order to explain the long-term periodic variability of the accretion rate, CG 01 proposed a hierarchical triple stellar model, in which a distant tertiary exerts tidal forces on the inner binary. This results in a cyclic exchange of the angular momentum between the inner system and the tertiary (Kozai 1962; Lidov & Ziglin 1976; Mazeh & Shaham 1979; Bailyn & Grindlay 1987; Ford, Kozinsky & Rasio 2000, hereafter F 00; Bailyn, Lee & Socrates 2002; Wen 2003, hereafter W 03). The period of the resulting evolution of the parameters of the system is  $P_2^2 = P_1$ , where  $P_2$  is the orbital period of the tertiary, implying  $P_2 = 1$  d. The variable system parameter relevant here is the eccentricity,  $e_1$ , of the inner system, which causes changes of the distance be-

tween the inner Lagrange point,  $L_1$ , and the center of mass of the secondary. This in turn changes the rate of the flow through  $L_1$  and the accretion rate. The mass of the tertiary has been constrained by CG 01 as  $M_3 < 0.5M_\odot$  based on the lack of its optical detection. We note that this constraint assumes the third body is a main-sequence star; if it is a white dwarf or a neutron star,  $M_3 < 1.4M_\odot$ . (Still, the third star is most likely on the main sequence, which we assume hereafter.) However, no specific calculations of the proposed triple system, e.g., of the maximum  $e_1$  from modelling the variable rate of the flow through the  $L_1$  point, or of the system parameters from modelling gravitational evolution of the system, have been done yet.

Here, we first analyse the RXTE ASM monitoring data and the Proportional Counter Array (PCA) scanning data, and use them to quantify the source X-ray variability. We then present calculations on the dependence of the accretion rate through  $L_1$  on the eccentricity, which yields the maximum  $e_1$  required to reproduce the observed amplitude of the superorbital variability. Then, we model evolution of hierarchical triple stellar systems, and reproduce the 170-d period and the maximum eccentricity implied by the  $L_1$ -flow model. Our results put constraints on the masses of the system component, the inclination between the inner and outer orbits, and the ratio between its semi-major axes. We also report a discovery of a remarkable synchronization between the superorbital period and the period of the relativistic periastron precession of the binary.

## 2 THE DATA

Fig. 1 shows the long-term light curve of 4U 1820-303 from the RXTE ASM (1996 January 1-2007 January 4). For the clarity of display, we have averaged some adjacent 1-day measurements in order to achieve the minimum significance of 3 of the plotted count rate. We clearly see the cyclic variations of the count rate on the 170-d quasi-period with a large relative amplitude. The vertical lines show the predicted minima according to the ephemeris of eq. (9) of CG 01. Using the Lomb-Scargle periodogram (Lomb 1976; Scargle 1982), we find that the present (daily-averaged) ASM data yield  $P_3 = 170.6 \pm 0.3$  d, compatible with the periods of CG 01 and of W 06.

Fig. 2(a) shows the ASM light curve folded on the ephemeris of CG 01, as well as the folded light curve averaged over 10 phase bins. We see that while the daily measurements span a factor  $> 10$ , the averaged light curve varies over the superorbital period spanning a factor of 2.

We also use the available Galactic bulge scan data<sup>1</sup> from the RXTE PCA detector for the time interval of 1999 February 5-2006 October 30. Fig. 2(b) shows the count rate from those measurements folded, and folded over the superorbital ephemeris. We also show the count rate folded and averaged over 10 phase bins. Similarly to the ASM data, we see that while the individual measurements of the count rate span a factor of 10, the averaged light curve varies over the superorbital period spanning a factor of 2. We stress, however, that

<sup>1</sup> [http://heawww.gsfc.nasa.gov/users/craigm/galscan/htm/1/4U\\_1820-30.htm](http://heawww.gsfc.nasa.gov/users/craigm/galscan/htm/1/4U_1820-30.htm)

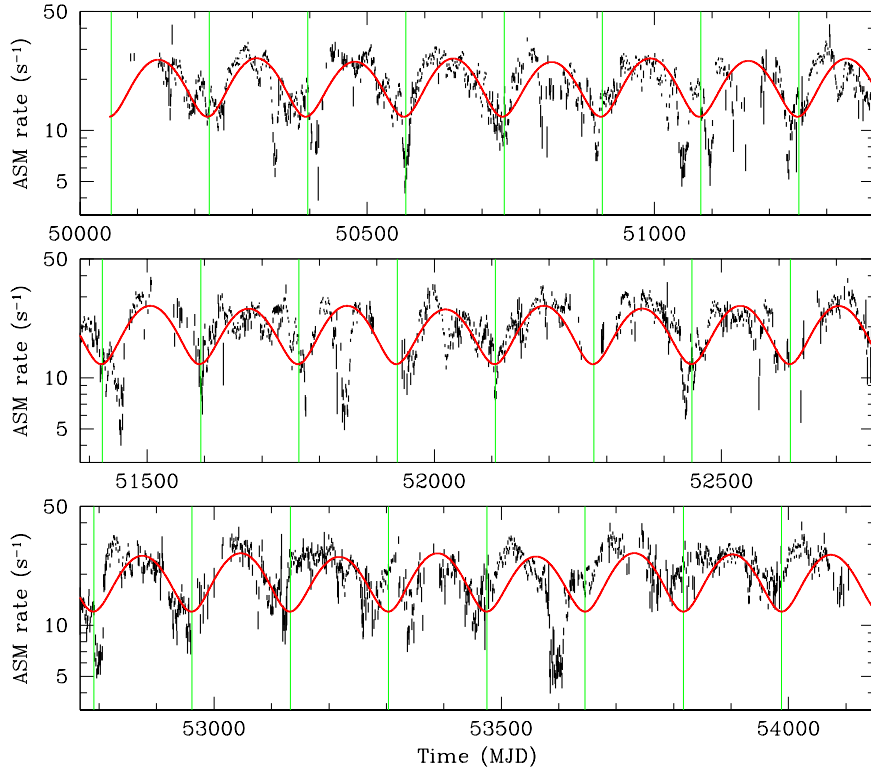


Figure 1. The RXTE/ASM light curve based on 1-day average measurements. The vertical lines show the minimum of the superorbital cycle according to the ephemeris of CG 01. Note departures of the ASM minimum from the predicted dates up to 50 d in some cases, as well as secondary minima (see also Simon 2003). The solid curve presents our theoretical model of Sections 3(4).

the variability is not strictly periodic, and  $P_3$  represents only a quasi-period. Therefore, folding and averaging over a single period value results in some suppression of the actual average superorbital variability. With that caveat, we attribute the changes of the average flux within the factor '2' to a relative stable quasi-periodic process (Sections 3(4)), and the remaining variability to some aperiodic processes, in particular those operating in other atoll sources. We also assume that the ASM and PCA count rate variability reflects that of the accretion rate, and assume hereafter its superorbital variability consists of variations within  $(0.7\{1.4\})h M_{-2}$ .

ZGW 07 have, in addition, analyzed available PCA and High Energy X-ray Timing Experiment (HEXTE) pointed observations of 4U 1820{303. Using a physically-motivated spectral model, they have estimated the bolometric flux from the source for each observation. The resulting light curve, when folded over the ephemeris, is very similar to those of Fig. 2. In particular, the fractional variability of the folded/averaged light curve is also found to be  $\sim 2$ . Since the bolometric flux is highly likely to be proportional to the rate of accretion onto a neutron star, that result confirms that the superorbital range of  $M_{-2}$  is indeed within a factor of 2, as adopted above.

### 3 THE MASS FLOW THROUGH THE INNER LAGRANGIAN POINT

Here, we calculate the dependence of the rate of the Roche lobe overflow (assumed to equal the accretion rate) on the

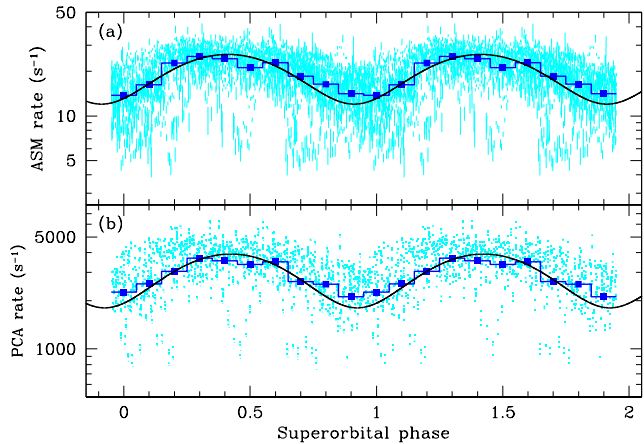


Figure 2. (a) The ASM light curve of Fig. 1 folded on the superorbital ephemeris of CG 01. (b) The folded light curve for the PCA Galactic bulge scan data (see Section 2). On each panel, the histogram shows the light curve averaged over 10 phase bins, and the solid curve shows the theoretical model of Sections 3(4) (based on the second cycle of Fig. 4a) fitted to the averaged data.

eccentricity. For that, we follow classical results on the Roche lobe, expressing  $M_{-2}$  as the product of the density and the sound speed at the inner Lagrangian point,  $L_1$ , times an effective area of the flow. The position of the  $L_1$  varies with the orbital phase in an eccentric orbit, yielding a varying  $M_{-2}$ . This yields the orbit-averaged  $M_{-2}$  as a function of the eccentricity,  $e_1$ . This in turn allows us to determine the mass-

in um eccentricity,  $e_{\text{max}}$ , required to enhance  $M_2$  ( $e$ ) by the factor of two inferred above from the varying  $F_{\text{bol}}$ , assuming that the minimum of the superorbital cycle correspond to the  $e_1$  minimum of  $e_0 = 0$ .

We first briefly estimate the parameters of the inner binary. We assume that the white dwarf fills its Roche lobe. Then, we combine the volume-averaged Roche-lobe radius for  $M_2 = M_{12} < 0.8$  of Paczynski (1971),

$$\frac{R_2}{a_1} = \frac{2}{3^{4/3}} \frac{M_2}{M_{12}}^{1/3}; \quad (1)$$

with the Kepler law,

$$a_1^3 = GM_{12} \frac{P_1^2}{4^2}; \quad (2)$$

where  $G$  is the gravitational constant,  $a_1$  is the semi-major axis, and  $M_{12} = M_1 + M_2$ . This yields the relation,

$$P_1 = \frac{9}{2^{1/2}} \frac{R_2^{3/2}}{(GM_2)^{1/2}}; \quad (3)$$

We then use the mass-radius relation for cold, low-mass stars of Zapolsky & Salpeter (1969; as fitted in R87), and assume pure He and the radius equal that of the fully degenerate con guration times a factor  $f_d = 1.1 - 0.1$  (R87). This yields  $M_2 \approx 0.067^{+0.10}_{-0.10} M_{\odot}$  and  $R_2 \approx 2.19^{+0.10}_{-0.11} 10^8 \text{ cm}$ , where the lower and upper limits correspond to  $f_d = 1$  and 1.2, respectively. For a star approximated by an  $n = 3/2$  polytrope (Chandrasekhar 1939),

$$R_2 \approx 0.0128(1 + X)^{5/3} \frac{M_2}{M}^{1/3} R; \quad (4)$$

where  $X$  is the H mass fraction, combined with equation (3) yields  $M_2 \approx 0.067 M_{\odot}$  and  $R_2 \approx 2.19 \cdot 10^8 \text{ cm}$  at  $X = 0.1$ . Then  $a_1 \approx 1.29 \cdot 10^8 (M_{12} = 1.35 M_{\odot})^{1/3} \text{ cm}$ , where we used  $M_{12} = 1.35 M_{\odot}$  corresponding to the presence of the resonance implied by equation (35) below, which then yields  $M_1 \approx 1.28 M_{\odot}$ .

For those parameters, and assuming negligible effects of a possible outow, eq. (17) of R87 yields the average mass transfer rate of  $h M_{2-i} \approx 3.5^{+1.1}_{-0.9} \cdot 10^7 \text{ g s}^{-1}$  (where the lower and upper limits correspond to  $f_d = 1, 1.2$ , respectively). This rate is fully compatible with the accretion rate,  $\approx (3.3 - 0.1) \cdot 10^7 \text{ g s}^{-1}$  (where the error is statistical only), corresponding to the average bolometric flux measured using the pointed RXTE PCA/HEXTE observations,  $\approx (8.7 - 0.2) \cdot 10^9 \text{ erg cm}^{-2} \text{ s}^{-1}$  (ZGW 07) at  $D = 7.6 \text{ kpc}$  and an accretion efficiency of 0.2. Using  $M_1 = 1.4 M_{\odot}$  increases the above theoretical rate by 0.2  $\text{g s}^{-1}$ . In our numerical estimates below, we use  $M_1 = 1.28 M_{\odot}$ ,  $M_2 = 0.07 M_{\odot}$ ,  $R_2 = 2.2 \cdot 10^8 \text{ cm}$ , and the corresponding  $h M_{2-i} = 4 \cdot 10^7 \text{ g s}^{-1}$ .

The distance,  $R_0$ , between the center of the white dwarf and the  $L_1$  point at  $e_1 = 0$ , is given by the solution of

$$(1 - x)^2 - (1 + x) = \frac{M_2}{M_1} (x^2 - x); \quad (5)$$

where  $x = R_0/a_1$ , which yields  $R_0 \approx 0.237a_1 \approx 3.05 \cdot 10^8 \text{ cm}$ . At  $e_1 = 1$ , the  $L_1$  distance is proportional to the separation, i.e., it equals  $R_0 + d^0$ , where

$$d^0 = R_0 e_1 \frac{e_1 + \cos \theta}{1 + e_1 \cos \theta}; \quad (6)$$

is the orbital angle with respect to the periastron, and  $d^0 = R_0$  changes between  $e_1$  and  $e_0$ . (See Brown & Boyle 1984 for an expression valid at large  $e_1$ .)

The rate of the Roche lobe overflow can be generally written as (e.g., Savonije 1983),

$$M_{2-i} = A c_s; \quad (7)$$

where  $A$  is an effective area of the overflow, and  $c_s$  are the mass density and the isothermal sound speed,  $c_s = (kT = m_H)^{1/2}$ , respectively, at  $L_1$ , and  $m$  is the mean molecular weight. Thus,  $M_{2-i}$  depends on the depth of the  $L_1$  point within the donor star,  $d$ . It can be shown by expanding the effective gravitational potential around  $L_1$  that

$$A \approx \frac{P_1^2}{2} \frac{GM_2}{R_0^2} d; \quad (8)$$

(Savonije 1983). Note that distinguishing here between the radius of the  $L_1$  point,  $R_0$ , and the volume-averaged radius of the star filling the Roche lobe,  $R_2$ , would require much more complex treatment of the overflow than that adopted here.) Paczynski & Sienkiewicz (1972) find that in the polytropic case  $M_{2-i} / d^{1.5+n}$ , where  $n$  is the polytropic index [which can be shown to follow from equations (7)-(8)]. If we neglect for a while the illumination of the white dwarf by the X-ray source, the relevant index would be  $n = 3.25$  of the (non-degenerate) surface layers of the white dwarf (Schwarzchild 1958). Then, the orbital-angle dependent accretion rate in an elliptical orbit can be written as,

$$M_{2-i} (e_1) = M_{2-i} \frac{m_{\text{ax}} (d_0 + d^0; 0)}{d_0}^{4/5}; \quad (9)$$

where  $d_0$  and  $M_{2-i}$  (assumed hereafter = 0.7h  $M_{2-i}$  corresponding to the minimum of the average light curves of Fig. 2, see Section 2) are the depth of the  $L_1$  point and the accretion rate, respectively, at  $e_1 = 0$ .

Assuming arbitrarily the white dwarf luminosity of  $10^3 L_{\odot}$ , using the metal abundance of  $Z = 0.01$  of NGC 6624 given by Rich, Manni & Liebert (1993),  $m_{\text{ax}} = 4/3$  for ionized He, and  $T(d) = (d)$ , and the (very approximate) Kramers' opacity of Schwarzchild (1958), we find from equations (7)-(8) that  $d_0 \approx 1.64 \cdot 10^3 R_0$ . Note that this is much less than the typical thickness of the surface layer of  $0.01 R_2$  (Schwarzchild 1958). The orbit-averaged accretion rate and its dimensionless form are,

$$M_{2-i} (e_1) = \frac{1}{2} M_{2-i} (e_1) d; \quad m_{\text{ax}} = \frac{M_{2-i} (e_1)}{M_{2-i}}; \quad (10)$$

respectively. Given the high power in equation (9), we find that even a very low  $e_{\text{max}} \approx 8 \cdot 10^{-4}$  is sufficient to increase

$M_{2-i}$  by a factor of 2. Fig. 3(a) shows  $M_{2-i} (e_1) = M_{2-i}$  of equation (9) at this  $e_1$ . Fig. 3(b) shows the  $m_{\text{ax}}$  of this model. We see that  $m_{\text{ax}}$  increases initially, at low values of  $e_1$ , very slowly. Thus, our assumption that  $M_{2-i}$  corresponds to  $e_1 = 0$  (see above) introduces only a slight error as long as  $e_{\text{max}} \approx e_0$ . On the other hand, we note that we have used here the structure of an isolated white dwarf, while the gravitational field close to  $L_1$  is obviously affected by the gravity of the neutron star. This wouldatten the density profile and lead to a requirement of a higher  $e_{\text{max}}$ .

Moreover, the white dwarf is very close to the X-ray source, and thus it is irradiated. Irradiation could be avoided

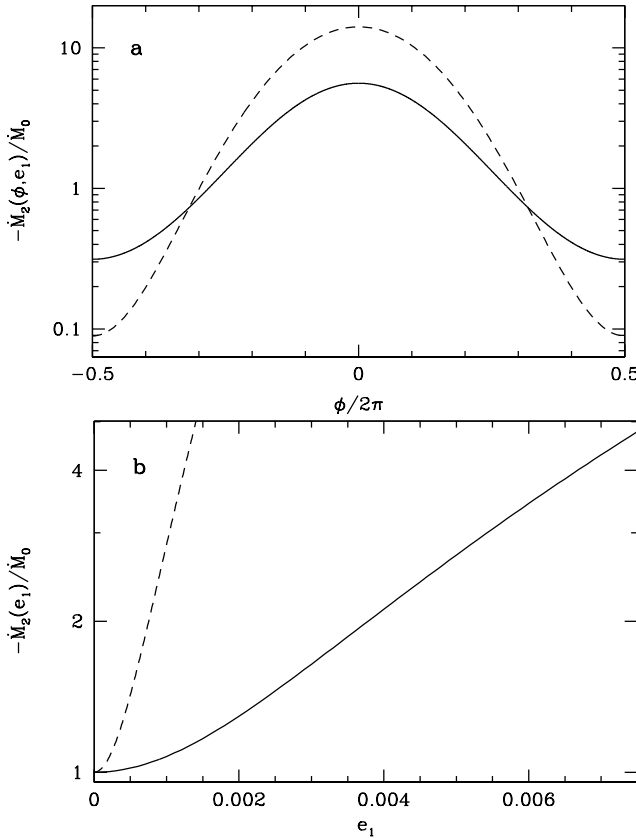


Figure 3. (a) The dashed and solid curves show the orbital phase dependence of the accretion rate for the model without irradiation at  $e_1 = 8 \cdot 10^{-4}$  and  $d_0 = R_0 = 1.64 \cdot 10^3$ , equation (9), and with irradiation at  $e_1 = 4 \cdot 10^{-3}$  and  $H_0 = R_0 = 2.3 \cdot 10^3$ , equation (13), respectively. The periastron corresponds to  $\phi = 0$ . In both cases,  $m_e \approx 2$ , illustrating the orbital phase dependence of  $M_2$  at the respective  $e_{\text{max}}$  required to explain the superorbital cycle of 4U 1820{303. (b) The dashed and solid curves show the orbital-averaged accretion rate,  $m_e$ , as function of  $e_1$  for the two above models, respectively.

if the accretion disk were strongly shaded and obscured the white dwarf from the X-ray source. However, the observed strong orbital modulation in the UV (Anderson et al. 1997) is well explained by reprocessing of X-rays by the white dwarf (Arons & King 1993), which interpretation rules out strong shading. Thus, we consider now the case with irradiation of the white dwarf.

The white dwarf subtends the solid angle  $\Omega = R_2^2/a_1^2$ , which, for our binary parameters, is  $\approx 7.3 \cdot 10^{-3}$ . For the  $H_{\text{bol}}$  and an albedo of 0.5 (e.g., Anderson 1981; London, McCray & Auer 1981), the white dwarf receives  $2.2 \cdot 10^{35}$  ( $D = 7.6 \text{ kpc}$ ) $^2 \text{ erg s}^{-1}$ , i.e., several orders of magnitude more than its possible intrinsic luminosity. The absorbed flux per unit area at a mid-point of the white dwarf (at a  $\phi = 0$  from the neutron star) varies then in the range  $F_{\text{irr}} \approx (0.9 \pm 1.8) \cdot 10^6$  ( $D = 7.6 \text{ kpc}$ ) $^2 \text{ erg cm}^{-2} \text{ s}^{-1}$ . This variability is due to the X-ray luminosity undergoing the superorbital cycle with the amplitude of 2. The corresponding blackbody temperature changes from  $T = T_0 \approx 1.1 \cdot 10^6$  ( $D = 7.6 \text{ kpc}$ ) $^{1/2}$  K to  $2^{1/4} T_0$ . Assuming  $L \propto m_e$ ,  $T(e) = m_e^{1/4} T_0$ . In optically-thick regions, the structure of the atmosphere will be closely isothermal at this  $T$  (e.g.,

Anderson 1981). Thus, the atmosphere density will decrease exponentially with the distance from the center of the white dwarf,  $\rho \propto \exp(-d/H)$ , where  $H$  is the scaleheight around the  $L_1$  point,

$$\frac{H}{R_0} \approx \frac{c_s^2 R_0}{GM_2} \approx 2.3 \cdot 10^3 m_e^{1/4} \frac{T_0}{1.1 \cdot 10^6 \text{ K}}; \quad (11)$$

where we used our numerical values of the parameters for the second equality. Then, we use the results of Brown & Boyle (1984), who derived  $A \approx (2)^{1/2} H R_0$  (see their eq. 4), which can be expressed as,

$$M_2(e_1) \approx (2)^{1/2} t_{\text{dyn}}^2 c_s^3 \rho_0 \exp(d/H); \quad (12)$$

where  $t_{\text{dyn}} = (R_2^3/GM_2)^{1/2} \approx 55 \text{ s}$  is close to the dynamical time scale of the white dwarf [ $(R_2^3/GM_2)^{1/2} \approx 30 \text{ s}$ ], and  $\rho_0$  is the atmosphere density at  $L_1$  corresponding to  $e_1 = 0$ . Here we neglected the correction of Brown & Boyle (1984) for the velocity of the  $L_1$  point, since it is much slower than the sound speed in our case. Note that though the functional dependence  $\rho \propto c_s^3 \rho_0$  is most likely accurate, the constant of the proportionality remains relatively uncertain (see Savonije 1983) as well as the argument of the exponent may be more complex than that used above, see Frank, King & Raine (2002), pp. 352{353. The latter effect may increase the scaleheight around  $L_1$  and thus lead to a requirement of a higher  $e_{\text{max}}$  than that estimated by us below. To solve this problem accurately, hydrodynamical simulations (see, e.g., Regos, Bailey & Mandling 2005) specific to 4U 1820{303 (beyond the scope of this work) are needed.

The  $H$  and  $c_s$  depend on  $e_1$  through  $T(e_1)$ , and we denote their values at  $e_1 = 0$  as  $H_0$  and  $c_{s0}$ , respectively. The accretion rate relative to that at  $e_1 = 0$  can then be written as,

$$\frac{M_2(e_1)}{M_2(0)} \approx m_e^{3/8} \exp \left( \frac{e_1 R_0}{H_0 m_e^{1/4}} \frac{e_1 + \cos \phi}{1 + e_1 \cos \phi} \right); \quad (13)$$

This equation coupled with equation (10), giving  $m_e$ , can be easily solved iteratively.

This solution, for a given  $H_0 = R_0$ , can be used to calculate the eccentricity required for a given amplitude of  $L$ . Fig. 3(a) shows an example of the dependence of equation (13) for  $e_1 = 0.004$  and  $H_0 = R_0 = 0.0023$ , yielding  $m_e \approx 2$  (i.e.,  $e_{\text{max}} \approx 0.004$ ). Fig. 3(b) shows  $M_2(e_1)$  for the same  $H_0 = R_0$ . In general, the accretion rate enhancement due to the eccentricity depends primarily not on  $e_1$  itself but on  $e_1 = (H_0/R_0)$ . In particular, the eccentricity required to obtain the increase of the orbit-averaged accretion rate by 2 is  $e_{\text{max}} = 2H_0 = R_0$ . We also note that the value of  $e_{\text{max}}$  does not depend on the (relatively uncertain) normalization of the  $M_2$  dependence of equation (12).

From that normalization, we can determine  $\rho_0$  as,

$$\rho_0 = \frac{M_2(0)}{(2)^{1/2} t_{\text{dyn}}^2 c_{s0}^3} \approx 2.0 \cdot 10^6 \text{ g cm}^{-3}; \quad (14)$$

This corresponds to an electron density of  $n_e \approx 6.0 \cdot 10^{17} \text{ cm}^{-3}$ , and the Thomson optical depth above the  $L_1$  of 1.0. The Rosseland absorption opacity at the above  $T \approx 1.1 \cdot 10^6 \text{ K}$  and  $Z = 0.01$  is  $\approx 17 \text{ g}^{-1} \text{ cm}^{-2}$  (Iglesias & Rogers 1996), i.e.,  $\approx 10^3$  more than the scattering opacity for He. Thus, the medium is completely optically thick, consistent

with our assumption of the temperature equal to the black-body one. The corresponding pressure is  $10^7 \text{ dyn cm}^{-2}$ , which can be calculated to be  $10^7 \text{ cm esm}$  more than the critical pressure below which a transition to an optically thin regime begins (London et al. 1981). Note that the  $L_1$  region may be partly shadowed by the accretion disc, which would decrease the temperature and move the  $L_1$  region even more into the optically-thick regime. We also check that the time scale at which the atmosphere locally responds to the irradiation,  $2n_0 k T_0 H_0 = F_{\text{irr}} / 15 \text{ ms}$ , is much shorter than any other time scale of interest.

On the other hand, the coefficient in equation (12) and other details of the flow through  $L_1$  are relatively uncertain, and thus it is of interest to also consider the case with the  $L_1$  region being optically thin. Above a transition zone (Anderson 1981; London et al. 1981), the atmosphere temperature becomes close to the Compton temperature of the surrounding radiation field (e.g., Kallman & McCray 1982; Begelman, McKee & Shields 1983),

$$T_c = \frac{h J d}{4k J d} \quad (15)$$

where  $J$  is the mean intensity. For the sum of the X-ray spectrum of the source, its reflection from the star, and the blackbody emission from reprocessing in the underlying regions of the star,  $T_c$  will be  $2-3$  of the Compton temperature of the star,  $T_c$  will be  $2-3$  of the Compton temperature for the X-ray spectrum alone. Based on the spectra of ZG W 07, we have calculated the latter to range from  $(1.6 \pm 1.8) \times 10^7 \text{ K}$  in the high-luminosity state to  $10^8 \text{ K}$  in the low-luminosity state. Thus,  $T_c = 10^7 \text{ K}$  for the dominant high-luminosity state. As the Compton temperature depends only on the shape of the spectrum but not on its flux,  $T_c$  is almost independent of  $M_2$ , except for the lowest  $M_2$  corresponding to the hard low state, where  $T_c$  is several times higher. Neglecting the last effect (important only at the flux minimum), equation (11) yields  $H = R_0 / 0.2$ .

If this condition were dominant over the superorbital cycle, a very high  $e_{\text{max}} = 0.4$  would be required to account for the superorbital variability. Then  $L_1$  point would move by  $0.4R_0$  below its position at  $e_1 = 0$ . If the moving  $L_1$  point is to remain in the optically thin regime, the degenerate interior of the white dwarf could obviously not fill the Roche lobe, as the  $L_1$  at  $e_1 = 0$  would have to be 2 scaleheights above the degenerate surface. Otherwise, the  $L_1$  around the periastron would penetrate within the very dense degenerate medium, which would result in a catastrophic mass loss and disruption of the star. (Cf. calculations of Regos et al. 2005, where a very fast mass loss occurs above a critical  $e_1$  at which the  $L_1$  touches the surface at the periastron.) Such a white dwarf would be much heavier (probably close to the maximum mass,  $1.4M_\odot$  and the minimum radius,

$5 \times 10^8 \text{ cm}$ ), which would then lead to an increase of the accretion rate by approximately the square of the relative mass increase (see, e.g., formulae in R87), which appears to be in conflict with the data. Furthermore, it appears then impossible to start the mass transfer. However, we stress that our estimates do not require the  $L_1$  region of the irradiated star to be in the optically thin regime, but rather, given the above, rule it out.

Still, we cannot rule out that the  $L_1$  point is in the transition zone (Anderson 1981; London et al. 1981) between  $T_c = 10^5 \text{ K}$  and  $10^7 \text{ K}$ , in which case detailed solutions

of the atmosphere structure would be required to calculate  $M_2(e_1)$ , and the  $e_{\text{max}}$  would be somewhat higher than the value of 0.004 estimated above. On the other hand, the shadowing of the white dwarf by the disc would (as mentioned above) decrease the temperature of the  $L_1$  region. These effects introduce some systematic uncertainties on the value of  $e_{\text{max}}$ .

#### 4 MODELS OF THE TRIPLE SYSTEM

Above, we have modelled the accretion rate variability in 4U 1820-303 as due to variability of the binary eccentricity. Here, we model the required variability of the eccentricity as due to gravity of a third star in the system. The third star should have the semi-major axis ( $a_2$ ; measured with respect to the center of mass of the inner binary) satisfying  $a_2 = a_1 / 1$  in order not to perturb the binary motion on time scales in the range between  $P_1$  and  $P_3$ , which perturbations have not been observed. Thus, this model is of a hierarchical triple system. We then attempt to reproduce the observed 171-day period and its relative coherence (Section 2) as well as the eccentricity amplitude necessary to reproduce the observed amplitude of the superorbital variability as inferred from our  $L_1$ -flow calculations (Section 3).

We begin with a brief review of the main features of secular effects in hierarchical triple systems. It has been known (e.g., Ozai 1962) that a third outer body can induce quasi-periodic oscillations of the inner eccentricity with a long quasiperiod of

$$P_3 = K \frac{P_2^2}{P_1}; \quad (16)$$

where  $P_2$  (the outer orbital period) is given by

$$P_2^2 = \frac{4 \pi^2 a_2^3}{GM}; \quad (17)$$

$M = M_1 + M_2 + M_3$ , and  $K$  (often  $\approx 1$ ) depends on the system parameters. There are two main regimes. At an initial mutual inclination,  $i_0$ , above a critical angle,  $i_c \approx 40^\circ$ , the amplitude of the inner eccentricity is large and  $K \approx 1$ . The evolution can be well described by taking into account only the lowest-order perturbative term in the system Hamiltonian expanded in powers of  $a_1 = a_2$ , namely the quadrupole term,  $\propto (a_1 = a_2)^2$ . Then, the mutual inclination,  $i$ , is anticorrelated with the inner eccentricity,  $e_1$ , with  $(1 - e_1^2) \cos^2 i$  constant. In this approximation, both semi-major axes, the outer eccentricity,  $e_2$ , and the magnitude of the angular momentum of the outer binary are constant, and there is exchange of the angular momentum between the inner and outer binary. In a conservative system, also the total angular momentum and energy are constant. The maximum inner eccentricity is roughly  $e_{\text{max}} \approx [1 - (5/3) \cos^2 i_0]^{1/2}$  (Innanen et al. 1997; Holman, Touma & Tremaine 1997) above the critical angle (and thus  $e_{\text{max}} \approx 1$  for  $i_0 \approx 90^\circ$ ).

Below  $i_c$ ,  $e_{\text{max}} \approx 1$ , and the quadrupole approximation becomes insufficient. In particular, for coplanar orbits,  $i_0 = 0$ , the quadrupole term in the Hamiltonian becomes null, and the first non-zero term is octupole,  $\propto (a_1 = a_2)^3$ . In the octupole approximation, only the semi-major axes are constant [?] (apart from the total energy and angular momentum). In this regime, the inner eccentricity also varies

quasi-periodically, but at a period longer [?] than that of the quadrupole one. In the intermediate regime where both terms are important, time dependencies of the inner eccentricity show both periodicities (Krymowksi & Mazeh 1999). Also, at  $e_{\text{max}} = 1$  in general,  $e_{\text{max}}$  decreases with the increasing  $a_2 = a_1$ , increases with the increasing the initial outer eccentricity,  $e_{2,0}$ , and it depends very weakly on either  $M_3 = M_{12}$  or  $M_2 = M_1$  (F00).

We use a numerical model calculating the time evolution of an isolated hierarchical triple of point masses, using secular perturbation theory up to the octupole terms (e.g., F00; Miller & Hamilton 2002; Baes et al. 2002; W03). We neglect possible effect of the tidal deformation of the white dwarf on the gravitational force exerted on the inner binary, see, e.g., Soderhjelm (1984), Eggleton & Kiseleva-Eggleton (2001). Also, the Hamiltonian is averaged over the periods of both the inner and outer binaries, and thus any possible short-time scale changes (e.g., Bailyn 1987; Georgakarakos 2002) are averaged out. Our calculations are Newtonian apart from the general relativistic (GR) periastron precession in the inner binary. Its first-order post-Newtonian period,  $P_{\text{PN}}$ , is given by (e.g., Weinberg 1973),

$$P_{\text{PN}} = \frac{P a c^2 (1 - \dot{e})}{3G M_{12}} = \frac{P_1^{5/3} c^2 (1 - \dot{e})}{3(2GM_{12})^{2/3}}; \quad (18)$$

We include this effect in the same way as in, e.g., W03.

The free parameters of the model are the masses of the neutron star,  $M_1$ , and of the third star,  $M_3$ ,  $a_2 = a_1$ ,  $i_0$ ,  $e_{2,0}$ , and  $e_0$ . We assume  $e_0 < e_{\text{max}} = 0.004$  (Section 3). Then, we know  $P_1$  and  $P_3$ , and assume  $M_2 = 0.07M_1$  (Section 3).

Given the relatively large number of free parameters and complex dependencies between them and the resulting period and the amplitude of the eccentricity modulation, it has proven difficult to constrain the parameter space numerically. Thus, we have obtained some approximate analytical constraints. Given the presence of only one, well-defined, long-term periodicity in the system (Section 2; W06), evolution of the triple system can be dominated by either the quadrupole or the octupole term, but not by both, which would have given rise to two periodicities (as noted above). Given the considerably greater simplicity of the quadrupole equations, we consider them for our analytical estimates (though we do include the octupole term in numerical calculations). Given our requirement of  $e_{\text{max}} = 1$ , this implies values of  $i_0$  close to  $i_c$ .

We first estimate the maximum eccentricity. We use the conservation of the total angular momentum and energy. The former gives us the mutual inclination,  $i$ , in terms of  $i_0$  and  $e_1$ , e.g., eq. (3) in Miller & Hamilton (2002). Then the (quadrupole) Hamiltonian gives the total energy. The minimum and maximum inner eccentricity corresponds to the inner periastron angle ( $g_1$ , measured from the intersection of the two orbits),  $g_1$ , of 0 and  $=2$ , respectively. Equating the Hamiltonian at those two angles and using  $i$  from the angular momentum conservation, gives, in the lowest (second) order of  $e_1$ ,

$$e_{\text{max}}^2 = \frac{4 + P_{\text{PN}} + 2 \cos i_0}{10 \cos^2 i_0} e_0^2; \quad (19)$$

where

$$P_{\text{PN}} = \frac{8GM_{12}^2 a_2^3 (1 - \dot{e}_{2,0})^{3/2}}{c^2 M_3 a_1^4}; \quad (20)$$

$$\frac{M_{12}^{3/2} M_3 a_2^{1/2} (1 - \dot{e}_{2,0})^{1/2}}{M_1^{1/2} M_2 a_1^{1/2}}; \quad (21)$$

In order for a solution with  $e_{\text{max}} = e_0$  to exist, the denominator in equation (19) should be nearly zero. Also, at  $a_2 = a_1$ , which we assume hereafter. Thus,

$$\cos^2 i_0 = \cos^2 i_c = \frac{6}{10} P_{\text{PN}}; \quad (22)$$

Note that this  $i_c$  is also the critical angle for the large  $e_{\text{max}}$  regime (see Baes et al. 2002), and it becomes the Newtonian critical angle when  $P_{\text{PN}} = 0$  (Kozai 1962). In the small  $e_1$  limit, the initial mutual inclination angle should be approximately equal to but slightly smaller than the critical value, which is different from the requirement for high  $e_{\text{max}}$  regime. The value of  $e_{\text{max}}$  is determined by how close  $i$  is to  $i_c$ .

For a solution of equation (22) to exist,  $P_{\text{PN}} < 6$  is required. Then, we have from equation (20),

$$\frac{a_2^3}{a_1^3} < \frac{3}{4} \frac{c^2 a_1 M_3}{4G M_{12}^{2/3}} (1 - \dot{e}_{2,0})^{3/2}; \quad (23)$$

For  $M_{12} > 1.5$ , the upper limit on  $M_3$  of 0.5M (CG01) and  $e_2^2 < 1$ ,  $a_2 = a_1 < 25$ . Note that the constraint of equation (23) is the same as that derived for the high- $e_1$  case [except for the  $(1 - \dot{e})^{3/2}$  factor, Baes et al. 2002]. It is related to the fact that the Newtonian regime corresponds to  $P_{\text{PN}} = P_3$ . Otherwise, the GR periastron precession decreases the amplitude of the Kozai oscillations of  $e_1$ , and leads to its disappearing in opposite limit. This is because the effect of the third body is a coherent summation of the tidal perturbations over many orbital periods, and the GR precession partly destroys this coherence (e.g., W03). In particular, this leads to a change of  $i_c$ , equation (22), reducing the high- $e_{\text{max}}$  regime.

Another constraint on the parameter space comes from the observed  $P_3 = 171$  d. The inner binary spends most of the time around  $g_1 = -2$ , at which  $dg_1/dt = 0$ . We thus write  $g_1 = -2 + \omega t$  with  $\omega = 1$  and expand the (quadrupole) evolution equations for  $e_1$  and  $g_1$  [e.g., eqs. (16)(17) in W03] to the first order in  $\omega$  and in the small- $e_1$  approximation. We then use equation (19) to express the results in terms of  $e_{\text{max}} = e_0$ , divide  $de_1/dt$  by  $dg_1/dt$ , and integrate over  $e_1$  from  $e_0$  to  $e_{\text{max}}$ . This yields the value of  $K$  [equation (16)] of

$$K = \frac{2^{5/2} f}{3} \frac{M}{M_3 (4 + P_{\text{PN}})} (1 - \dot{e}_{2,0})^{3/2} \frac{e_{\text{max}}}{e_0} \ln^{\frac{1}{2}} \frac{e_{\text{max}}}{e_0}; \quad (24)$$

where  $f$  is a fudge factor to compensate for the approximation we used in the derivation. We found empirically that  $f \approx 1$  are within a factor of two, and in our example described below,  $f \approx 1.1$ . Note also that the superorbital period is strongly dependent on  $e_0$ , on which the accretion rate depends very weakly (as long as  $e_0 \neq 0$ , Fig. 3b).

The following constraint on the total mass of the inner binary can be obtained using equations (16)(17), (20) and (24),

$$\frac{3(GM_{12})^{2/3} (2)^{5/3} P_3 e_0}{2^{1/2} P_1^{5/3} e_{\text{max}}^{1/2} (e_{\text{max}} = e_0)} = \frac{f P_{\text{PN}}}{4 + P_{\text{PN}}} \frac{M_{12}}{M}^{2/3}; \quad (25)$$

which (for the observed  $P_1$  and  $P_3$ ) can be solved for  $P_{\text{PN}}$  as,

$$P_N \cdot \frac{4}{0.274f M_{12} = M} \cdot \frac{2=3 \frac{e_{\text{max}}}{e_0} \ln^{\frac{1}{2}} \frac{e_{\text{max}}}{e_0}}{1} : \quad (26)$$

The constraint of  $P_N < 6$  then yields a relation between  $M_{12}$  and  $e_{\text{max}} = e_0$ ,

$$\frac{M_{12}}{M} < 0.067 \cdot \frac{f e_{\text{max}}}{e_0} \cdot \ln^{3=4} \frac{e_{\text{max}}}{e_0} : \quad (27)$$

At  $f = 1.1$ , it allows  $M_{12} > 1.5M$  provided  $e_{\text{max}} = e_0 > 5.5$ . Since the required relative amplitude of  $M_2$  of  $\sim 2$  can be achieved at any  $e_{\text{max}} = e_0 > 3$  (see the solid curve in Fig. 3b), this is only a very weak constraint, allowing practically any of the theoretically possible masses of the neutron star at modest values of  $e_{\text{max}} = e_0$ .

Equation (20) at  $P_N < 6$  also yields a constraint on  $M_3$ . If we assume  $M_{12} = 1.5M$  and that the system is hierarchical,  $a_2 = a_1 > 5$ , we obtain  $M_3 > 0.004M$  [see also equation (23)]. An independent relation follows from equations (16)(17) and (24),

$$\frac{M_3}{(1 - \frac{e_{2,0}^2}{2})^{3=2} M_{12}} = \frac{2^{5=2} a_2^3 P_1 e_{\text{max}}}{3 a_1^3 (4 + P_N) P_3 e_0} \ln^{\frac{1}{2}} \frac{e_{\text{max}}}{e_0} ; \quad (28)$$

which yields the same constraint of  $M_3 > 0.004M$  at  $e_{\text{max}} = e_0 > 7$ . Thus, even a very low-mass third body can still induce the required eccentricity oscillations in the inner binary.

We have not studied analytically constraints in the octupole-dominated regime (which regime has been considered, e.g., by Rasio 1994, 1995; F00; Georgakarakos 2002; Lee & Peale 2003). The octupole-dominated regime may possibly yield solutions with  $i_0 = 0$  (as compared to  $i_0 \neq 0$  in the quadrupole regime). However, even if such solution exists, our conclusion of only very weak constraints on the masses of the system components will remain unaffected. On the other hand, an important difference between solutions in the two regimes is the variability of the mutual inclination. In the quadrupole low- $e_1$  regime, the maximum change,  $i = i - i_0$ , is given by

$$i' = \frac{e_{\text{max}}^2 - e_0^2}{2} \cot i_0 ; \quad (29)$$

which implies only a very small change of  $i$  over the course of the superorbital cycle, e.g., about  $2.3^\circ$  at  $i_0 = 40^\circ$ ,  $e_{\text{max}} = 0.004$ . On the other hand, numerical results of F00 (g. 8) show  $i = 15^\circ$  in their example for the octupole regime, low- $e_1$  oscillations, for which  $i_0 = 15^\circ$ ,  $e_{\text{max}} = 0.001$ . Since the angular momentum is dominated by the outer binary,  $i$  is approximately equal to the inclination with respect to the constant axis of the total angular momentum, which, in turn, is related to the value of (in principle observable) the inclination of the inner orbit to the line of sight.

For assumed values of  $M_1, M_2, M_3, e_0, e_{\text{max}}$ , and with the observed  $P_1$  and  $P_3$ , the above equations can be used to find  $a_2$  and  $i_0$ . These approximate analytical solutions can be then re-tuned numerically. We present an example yielding  $P_3 = 171$  d within 1 per cent and  $e_{\text{max}} = 0.004$ , corresponding to our model of the accretion with irradiation (Section 3). Its parameters are  $M_1 = 1.29M$ ,  $M_2 = 0.07M$ ,  $e_0 = 10^{-4}$ ,  $M_3 = 0.5M$ ,  $a_2 = a_1 = 8.66$  (yielding  $P_2 = 0.17$  d),  $i_0 = 40.96^\circ$ ,  $e_{2,0} = 10^{-4}$ , corresponding to  $P_N = 0.22$ ,  $\alpha = 19$ , and  $K = 41$ . The initial values of the

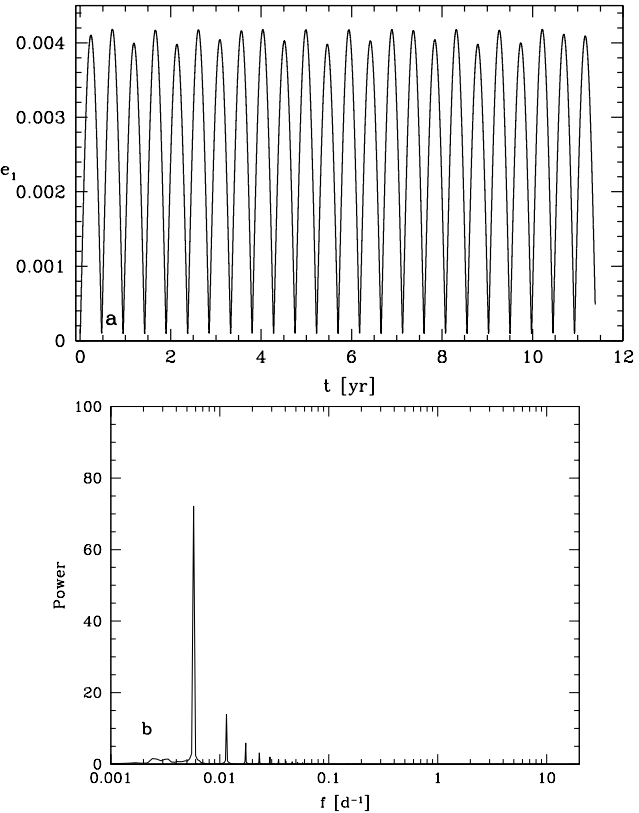


Figure 4. (a) The time evolution of the inner eccentricity,  $e_1$ , for our best model. (b) The Fourier power spectrum of the eccentricity dependence.

periaxis angles,  $g_1$  and  $g_2$ , are set to zero. Note that  $e_{\text{max}} = e_0$  is very sensitive to  $i_0$ , see equation (19).

The evolution of this model is shown in Fig. 4(a). Fig. 4(b) shows the Fourier power spectrum of  $e_1$  at the sampling rate of  $20 \text{ d}^{-1}$  (to approximate that of the RXTE/ASM). The  $P_3$  peak is unresolved at the resolution of the Fourier spectrum. This narrowness is similar to that observed, cf. g. 19 of W06. In Fig. 4(a), we also see a weak second quasi-periodicity, with the period slightly longer than twice of the main one. This is an effect of the octupole term in the evolution equations (see above).

We then use our results of Section 3 connecting  $e_1$  to  $M_2$ . We first apply equations (9)(10), yielding  $M_2(t)$  with the low parameters as in Fig. 3 to convert  $e_1(t)$  of Fig. 4(a) to  $M_2(t)$ . We multiply the model period by 0.987 in order to obtain the exact agreement with the observed  $P_3$ . We first plot the resulting  $M_2(t)$  (fitting only the normalization) by the solid curve in Fig. 1. We see that the model fits well the overall superorbital variability. We also note that the exact Newtonian calculations of the evolution would increase the scatter in  $e_1(t)$ , i.e., leading to a less periodic behaviour (e.g., F00). This could explain the presence of some observed superorbital cycles with a significantly different duration than the average  $P_3$  (see Fig. 1).

We then take the second cycle in Fig. 4(a) as representative and fit it to the average superorbital phase diagrams of Figs. 2(a,b), with the second free parameter being the phase offset (with respect to the ephemeris of CG01), which we find  $\alpha = 0.088$  and  $-0.076$  for the ASM and PCA

data, respectively. The  $t$  results, shown by the solid curves in Fig. 2(a{b), reproduce well the average phase diagram s.

## 5 LONG-TERM EVOLUTION AND OTHER CONSTRAINTS

Above, we have neglected the effects of emission of gravitational radiation (and of any other process of long-term loss of angular momentum) on the evolution of the inner binary. This is fully justified as we have considered evolution over the course of a decade, which is many orders of magnitude shorter than the time scale due to emission of gravitational waves. Thus, we can consider the long term evolution separately from the short-term one.

The time scale for the loss of the angular momentum,  $J_1$ , from the inner system due to emission of gravitational radiation is given by (Peters 1964),

$$g^1 = \frac{J_g}{J_1} = \frac{32}{5} \frac{2}{P_1} \frac{8=3}{c^5} \frac{M_1 M_2}{M_{12}^{1=3}} \frac{1+(7=8)e_1^2}{(1-e_1^2)^{5=2}} \quad (30)$$

$$' 1.23 \quad 10^6 \frac{M_1 M_2}{M_{12}^{5=3} M_{12}^{1=3}} \frac{P_1}{1s} \frac{8=3}{s^1} ; \quad e_1 \quad 1; \quad (31)$$

where

$$J_1 = M_1 M_2 \frac{G a_1 (1-e_1^2)^{1=2}}{M_{12}} : \quad (32)$$

This yields  $g' \approx 1:1 \times 10^7$  yr for our system parameters. We see that the effect of  $e_1 > 0$  on the rate of emission of gravitational radiation is negligible as long as  $e_1^2 \ll 1$ .

By logarithmically differentiating equation (32), assuming conservative mass transfer ( $M_1 = M_2$ ) and using equations (1{2) and (4), we can relate  $J_1$  to  $M_2$  and  $P_1$  (assuming a negligible  $e_1^2 \ll 1$ ),

$$\frac{J_1}{J_1} = \frac{M_2}{M_2} \frac{2}{3} \frac{M_2}{M_1} = \frac{P_1}{P_1} \frac{2}{3} \frac{M_2}{M_1} ; \quad (33)$$

where  $J_1$  includes all contributions to the inner angular momentum loss. Note that although the white dwarf expands as it loses mass, the accretion from  $M_2$  is not self-sustaining, i.e.,  $M_2 = 0$  if  $J=0$ , as well as it can take place only for  $M_2=M_1 < 2=3$ . Also,  $P_1=P_1 = M_2=M_2 > 0$ . This is in conflict with the observations, showing  $P_1 < 0$  (see Section 1). We note here that taking into account a possible mass loss from the system cannot resolve this discrepancy. If a fraction,  $\epsilon$ , of the mass lost by the secondary is ejected from the system, we derive from equations (1{2) and (4),

$$\frac{P_1}{P_1} = \frac{M_2}{M_2} \frac{1}{1} \frac{M_2}{M_{12}} : \quad (34)$$

Thus, although the mass loss reduces  $P_1$ , it is still  $> 0$ . Only in the absence of mass transfer, when the companion does not fill its Roche lobe, angular momentum losses (in particular, those due to gravitational radiation) lead to  $P_1=P_1 = 3J=J < 0$ . A possible resolution of this conflict is the apparent observed  $P_1 < 0$  resulting from gravitational acceleration of the system in the cluster potential (CG 01).

Then, the likely evolutionary scenario of 4U 1820{303 is still that of R 87, as shown on their g.1. According to it, the period shortly after the onset of the mass transfer ( $\sim 10^6$

yr ago) was  $\sim 500$  s. Then,  $a$  was lower and  $P_N$  higher [equation 20] than now. Consequently,  $\cos^2 i_c$  was less than the present value (i.e., the low- $e_{\text{max}}$ , octupole, regime was increased), see equation (22). Thus, the eccentricity oscillations had in the past lower amplitudes than now, and the system was in the octupole-dominated regime. On the other hand, a future increase of  $P_1$  may lead to  $i > i_c$  and moving the system to the high- $e_{\text{max}}$  regime (provided  $i < i_c$  at present). Then, the high eccentricity may lead to runaway mass transfer and tidal disruption of the secondary (see Section 3).

On the other hand, we find that at the present moment of the source evolution, the GR periastron precession period,  $P_{PN}$ , is very close, and may be equal exactly, to the superorbital period,  $P_3$ . Namely,

$$\frac{P_{PN}}{171 \text{ d}} = (1-e_1^2) \frac{P_1}{685 \text{ s}} \frac{5=3}{1:347M} \frac{M_{12}}{2=3} : \quad (35)$$

We consider this equality to be a very remarkable coincidence. There appears to be not any way in which the GR periastron precession could by itself (i.e., without the presence of a third star) affect the orbit-averaged accretion rate. Thus, the origin of the above equality can be either purely accidental or it may be due to some evolutionary processes not understood by us now. We note that F 00 find the presence of a resonance at  $P_{PN} \approx P_3$  manifesting itself as a peak in  $e_{\text{max}}$  (g. 14 in F 00). However, it is not clear how that resonance could lead to the synchronization of  $P_{PN} \approx P_3$ .

On the other hand, our results and those of R 87 do allow  $P_{PN} = P_3$  to be satisfied exactly. If this is the case and at  $M_2 \approx (0.06\text{--}0.08)M_\odot$ ,  $e_1 \approx 1$  (Section 3), the mass of the neutron star would be  $M_1 \approx (1.27\text{--}1.29)M_\odot$ . Remarkably, modelling of an X-ray burst of 4U 1820{303 by Shaposhnikov & T Tarchuk (2004) gives  $M_1 = 1.29^{+0.19}_{-0.06}M_\odot$ . Also, G Rindlay et al. (1984) have measured the total masses of low-mass X-ray binaries in globular clusters (including 4U 1820{303) and concluded that the initial neutron-star masses appear substantially less than  $1.4M_\odot$  on average. We also note that some low neutron-star masses have recently been measured with high precision, e.g.,  $1.250^{+0.005}_{-0.005}M_\odot$  for PSR J0737{3039B (Lyne et al. 2004), and  $1.18^{+0.03}_{-0.02}M_\odot$  for the neutron-star companion of PSR J1756{2251 (Faulkner et al. 2005). Given those results,  $M_1 = 1.28M_\odot$  in 4U 1820{303 appears entirely plausible.

We also note that although Arons & King (1993) proposed that  $M_1 = 2M_\odot$  if the initial mass of the white dwarf were  $0.6M_\odot$  and  $0.5M_\odot$  has been accreted, the calculations of R 87 imply a much lower initial mass and a short mass-transfer time interval, with only  $0.1M_\odot$  accreted. Then, Zhang et al. (1998) proposed that  $M_1 = 2.2M_\odot$  if the frequency of the upper kHz QPO at its apparent saturation at 1060 Hz were equal to the Keplerian frequency at the last stable orbit. However, van der K lis (2000) shows that there is no saturation in a more extensive data set. Also, current theoretical models of kHz QPOs do not postulate that frequency identification, and use it only to provide an upper mass limit (e.g., van der K lis 2000).

The presence of the third star may affect the system evolution only if it remains stable and is not disrupted by encounters with stars in the cluster. The triple system itself is stable if  $a_2 = a_1 > 2.8(1+M_3/M_{12})^{2=5}$  (Mardling & Aarseth

2001), which is clearly satisfied in our case, with  $a_2 = a_1 = 10$ ,  $M_{12} = 1.5M_{\odot}$  (Section 4), and  $M_3 < 0.5M_{\odot}$  (CG 01). Then, the encounter time scale has been estimated by Miller & Hamilton (2002) in the limit of domination of gravitational focusing, and we write it as

$$t_{\text{enc}} \approx 4 \times 10^8 \frac{4 \times 10^5 \text{ pc}^3}{n_{\text{GC}}} \frac{10^{11} \text{ cm}}{a_2} \frac{2M}{M} \text{ yr.} \quad (36)$$

Here,  $n_{\text{GC}}$  is the number density of stars, which we assume to be numerically equal to the mass density of  $4 \times 10^5 M_{\odot} \text{ pc}^{-3}$  in the core of NGC 6624 (Ivanova et al. 2005), and  $a_2 = 10^1 \text{ cm}$ ,  $M = 2M_{\odot}$  (Section 4). Thus,  $t_{\text{enc}}$  is much longer than the gravitational-radiation time scale, equation (31), but still shorter than the estimated total lifetime of the system of  $10^9 \text{ yr}$  (R 87). Thus, an encounter could have formed the triple system during the lifetime of 4U 1820-303, but it is stable on the current evolutionary time scale.

We also note that the angular momentum will also be lost from the system due to tidal dissipation within the secondary at  $e_1 > 0$ . This mechanism usually leads to circularization (and synchronization) of close binaries (e.g., Zahn 1977), but in our case the influence of the tertiary will force  $h_{12} > 0$  and continuous dissipation (Mazeh & Shaham 1979). The time scale for this process,  $t = J = J_T$ , is related to the circularization time scale. This, unfortunately, remains very uncertain for stars without convective envelopes, in particular white dwarfs (e.g., Zahn 1977), and it may be very long. Here, we consider the turbulent dissipation model of Press, Wijita & Smarr (1975), which probably gives the lower limit to the actual dissipation time scale in a white dwarf (Zahn 1977). Using the time scale of Press et al. (1975) and the approach of Mazeh & Shaham (1979), we obtain,

$$t = \frac{125}{121} \frac{(1 - e_1^2)^{11/2}}{e_1^3} \frac{a_1}{R_2} \frac{11}{K} \frac{R_T}{M_1^2 M_{12}^2} P_1; \quad (37)$$

where  $R_T$  is the effective Reynolds number, which we assume = 20 following Press et al. (1975), and  $K$  is a dimensionless factor of the mean turbulent viscosity,

$$K = \frac{14}{M_2 R_2^{11}} \int_0^{R_2} (r) r^{13} dr; \quad (38)$$

where  $(r)$  is the stellar density. We have calculated  $K = 0.0257$  for a polytrope with  $n = 3/2$ , appropriate for a low-mass white dwarf. For our system parameters, we find then  $t = 2300 \text{ yr}$  (where the average is over the superorbital cycle), which for  $h_{12}^{3/2} = 0.003$  becomes  $10^1 \text{ yr}$ . Thus, even if the dissipation is as fast as envisaged by Press et al. (1975), the process is completely negligible compared to the gravitational radiation. However,  $t < 9$  for  $h_{12}^{3/2} > 0.06$ .

On the other hand, the soft X-ray absorption towards the source is consistent with being caused entirely by the interstellar medium, with no evidence for any local component (Futamoto et al. 2004). This appears to rule out strong outflows from either the irradiated disc, the irradiated surface of the white dwarf, or, in particular, mass loss through the  $L_2$  point. At the mass ratio of the binary, the absence of the  $L_2$  mass loss by the Roche-lobe filling star imposes the constraint of  $e_{\text{max}} < 0.07$ , as calculated by Regos et al. (2005). This rules out  $h_{12}^{3/2} > 0.06$ . Thus, presently, the tidal dissipation appears not to be the dominant channel of angular momentum loss.

## 6 CONCLUSIONS

We have obtained the following main results.

1. Using the RXTE data, we have quantified the average amplitude of the superorbital variability of the source. We find that amplitude in the folded and averaged light curves to be by about a factor of two.

2. We have considered the model in which the superorbital variability is due to a third star inducing cyclic variations (Kozai 1962) of the eccentricity of the binary (as proposed by CG 01). We have studied the dependence of the rate of the Roche-lobe overflow on the eccentricity taking into account the strong irradiation of the white dwarf by the X-ray source (Fig. 3b). We find the amplitude of the eccentricity required to account for the variability of the accretion rate by the factor of two is  $e_{\text{max}} > 0.004$  (assuming the minimum of the eccentricity is close to null). However, systematic uncertainties of this model may somewhat change the actual value of  $e_{\text{max}}$ .

3. We reproduce the above maximum eccentricity of  $> 0.004$  and the observed superorbital period of 171 d in a detailed model of a hierarchical triple system. Our calculations are Newtonian except for inclusion of the GR periastron precession. We then convolve the obtained eccentricity light curve with our theoretical dependence of the accretion rate on the eccentricity and obtain a theoretical luminosity light curve. This theoretical light curve is compared to and found to be in a good agreement with the observed light curves from the ASM and PCA/HETE detectors, see Figs. 1-2.

4. We also study the parameter space allowed by the observational data, the  $e_{\text{max}} > 0.004$  constraint, and  $M_3 < 0.5M_{\odot}$  (CG 01). We obtain analytical solutions for the low-eccentricity Kozai oscillations in the regime dominated by the quadrupole terms of the evolution equations. We find the ratio of the semi-major axes to be  $< 25$ , which follows from the constraint that the GR periastron precession does not quench the Kozai eccentricity modulation. The masses of the system components are only weakly constrained. In particular, the canonical neutron-star mass of  $1.4M_{\odot}$  is allowed in this model. The mass of the third body is constrained as  $0.004 < M_3 < 0.5M_{\odot}$ .

5. We find that the period of the binary GR periastron precession is approximately equal (and it is allowed to be exactly equal) to the observed superorbital period (which equals the period of the Kozai eccentricity oscillations in our model). We find this to be a remarkable and puzzling example of synchronization in a physical system.

6. We obtain some other constraints on the system. The binary eccentricity has to be  $< 0.07$  from the apparent absence of the mass loss by the Roche-lobe filling white dwarf through the  $L_2$  point. The angular momentum loss due to tidal dissipation in the white dwarf is found to be negligible compared to the loss due to emission of gravitational radiation. Also, we find the theoretical mass transfer rate due to the angular momentum loss via gravitational radiation is in complete agreement with that corresponding to the average bolometric flux from this source (as measured by ZGW 07).

## ACKNOWLEDGMENTS

We thank M. Abramowicz, W. Domrowski, M. G. Gilfanov, P. Haensel, J. M. Kolińska and A. P. Yamatnykh for valuable discussions. This research has been supported in part by the Polish grants 1P 03D 01827, 1P 03D 01128 and 4T 12E 04727. LW acknowledges support by the Alexander von Humboldt Foundation's Sofja Kovalevskaja Program (funded by the German Federal Ministry of Education and Research). MG acknowledges support through a PPARC PDRF. We also acknowledge the use of data obtained through the HEASARC online service provided by NASA/GSFC.

## REFERENCES

Anderson L., 1981, *ApJ*, 244, 555  
 Anderson S. F., Margon B., Deutsch E. W., Downes R. A., Allen R. G., 1997, *ApJ*, 482, L69  
 Arons J., King I. R., 1993, *ApJ*, 413, L121  
 Bailyn C. D., 1987, *ApJ*, 317, 737  
 Bailyn C. D., Grindlay J. E., 1987, *ApJ*, 312, 748  
 Begelman M. C., McKee C. F., Shields G. A., 1983, *ApJ*, 271, 70  
 Blaes O., Lee M. H., Socrates A., 2002, *ApJ*, 578, 775  
 Blöser P. F., Grindlay J. E., Kaaret P., Zhang W., Smale A. P., Barret D., 2000, *ApJ*, 542, 1000  
 Brown J. C., Boyle C. B., 1984, *A & A*, 141, 369  
 Chandrasekhar S., 1939, *An Introduction to the Study of Stellar Structure*. Univ. of Chicago Press  
 Chou Y., Grindlay J. E., 2001, *ApJ*, 563, 934 (CG 01)  
 Cornelisse R., et al., 2003, *A & A*, 405, 1033  
 Done C., Gierlinski M., 2003, *MNRAS*, 342, 1041  
 Eggleton P. P., Kiseleva-Eggleton L., 2001, *ApJ*, 562  
 Faulkner A. J., et al., 2005, *ApJ*, 618, L119  
 Ford E. B., Kozinsky B., Rasio F. A., 2000, *ApJ*, 535, 385 (Erratum 2004, *ApJ*, 605, 966) (F00)  
 Frank J., King A., Raine D., 2002, *Accretion power in astrophysics*. 3rd ed., Cambridge Univ. Press  
 Futamoto K., Mitsuda K., Takei Y., Fujimoto R., Yamasaki N. Y., 2004, *ApJ*, 605, 793  
 Georgakarakos N., 2002, *MNRAS*, 337, 559  
 Gladstone J., Done C., Gierlinski M., 2007, *MNRAS*, submitted  
 astro-ph/0603126  
 Grindlay J., Gursky H., Schnopper H., Parsignault D. R., Heise J., Brinkman A. C., Schrijver J., 1976, *ApJ*, 205, L127  
 Grindlay J. E., Hertz P., Steiner J. E., Murray S. S., Lightman A. P., 1984, *ApJ*, 282, L13  
 Hasinger G., van der Klis M., 1989, *A & A*, 225, 79  
 Iglesias C. A., Rogers F. J., 1996, *ApJ*, 464, 943  
 Innanen K. A., Zheng J. Q., Mikkola S., Valtonen M. J., 1997, *AJ*, 113, 1915  
 Ivanova N., Rasio F. A., Lombardi J. C., Jr., Dooley K. L., Proulx Z. F., 2005, *ApJ*, 621, L109  
 Kalmán T. R., McCormick R., 1982, *ApJS*, 50, 263  
 Katz J. I., 1973, *Nat. Phys. Sci.*, 246, 87  
 Katz J. I., 1980, *ApJ*, 236, L127  
 Koziaki Y., 1962, *AJ*, 67, 591  
 Krymowski Y., Mazeh T., 1999, *MNRAS*, 304, 720  
 Kuulkers E., den Hartog P. R., int' Zand J. J. M., Verbunt F. W. M., Harris W. E., Cocchi M., 2003, *A & A*, 399, 663  
 Lachowicz P., Zdziarski A. A., Schwarzenberg-Czerny A., Pooley G. G., Kitamoto S., 2006, *MNRAS*, 368, 1025  
 Larwood J., 1998, *MNRAS*, 299, L32  
 Lee M. H., Peale S. J., 2003, *ApJ*, 592, 1201  
 Lidov M. L., Ziglin S. L., 1976, *Cel. M. eph.*, 13, 471  
 Lomb N. R., 1976, *Ap. & SS*, 39, 447  
 London R., McCormick R., Auer L. H., 1981, *ApJ*, 243, 970  
 Lyne A. G., et al., 2004, *Sci*, 303, 1153  
 Mandeling R. A., Aarseth S. J., 2001, *MNRAS*, 321, 398  
 Mazeh T., Shaham J., 1979, *A & A*, 77, 145  
 Miller M. C., Hamilton D. P., 2002, *ApJ*, 576, 894  
 Mitsuda K., et al., 1984, *PA SJ*, 36, 741  
 Paczynski B., 1967, *Acta Astr.*, 17, 287  
 Paczynski B., 1971, *ARA & A*, 9, 183  
 Paczynski B., Sienkiewicz R., 1972, *Acta Astr.*, 22, 73  
 Peters P. C., 1964, *Phys. Rev.*, 136, B1224  
 Press W. H., Wijita P. J., Smarr L. L., 1975, *ApJ*, 202, L135  
 Riedhorsky W., Terrell J., 1984, *ApJ*, 284, L17  
 Rappaport S., Nelson L. A., MacC P., Joss P. C., 1987, *ApJ*, 322, 842 (R87)  
 Rasio F. A., 1994, *ApJ*, 427, L107  
 Rasio F. A., 1995, *ASPC*, 72, 424  
 Regos E., Bailey V. C., Mandeling R., 2005, *MNRAS*, 358, 544  
 Rich R. M., Minniti D., Liebert J., 1993, *ApJ*, 406, 489  
 Savonije G. J., 1983, in *Accretion-driven stellar X-ray sources*, eds. W. H. G. Lewin & E. P. J. van den Heuvel, Cambridge, Cambridge Univ. Press, p. 343  
 Scargle D., 1982, *ApJ*, 263, 835  
 Schwarzschild M., 1958, *Structure and evolution of stars*. New York: Dover  
 Shakura N. I., Sunyaev R. A., 1973, *A & A*, 24, 337  
 Shaposhnikov N., Titaruk L., 2004, *ApJ*, 606, L57  
 Simon V., 2003, *A & A*, 405, 199  
 Smale A. P., Lochner J. C., 1992, *ApJ*, 395, 582  
 Soderhjelm S., 1984, *A & A*, 141, 232  
 Stella L., Riedhorsky W., White N. E., 1987, *ApJ*, 312, L17  
 van der Klis M., 2000, *ARA & A*, 38, 717  
 Verbunt F., 1987, *ApJ*, 312, L23  
 Weinberg S., 1973, *Gravitation and Cosmology: Principles and Applications of the General Theory of Relativity*. New York: Wiley  
 Wen L., 2003, *ApJ*, 598, 419 (W 03)  
 Wen L., Levine A. M., Corbet R. H. D., Bradt H. V., 2006, *ApJS*, 163, 372 (W 06)  
 Wijers R. A. M. J., Pringle J. E., 1999, *MNRAS*, 308, 207  
 Zahn J. P., 1977, *A & A*, 57, 383  
 Zapsolsky H. S., Salpeter E. E., 1969, *ApJ*, 185, 809  
 Zdziarski A. A., Gierlinski M., Wen L., 2007, *MNRAS*, submitted (ZG W 07)  
 Zhang W., Smale A. P., Strohmayer T. E., Swank J. H., 1998, *ApJ*, 500, L171